

Study of Amino Ligands Fixation to Macroporous Supports and Their Influence on Albumin Adsorption

CESAR G. GOMEZ, MIRIAM C. STRUMIA

Departamento de Química Orgánica, Facultad de Ciencias Químicas, (IMBIV-CONICET) Universidad Nacional de Córdoba, Haya de la Torre y Medina Allende, Edificio de Ciencias II - Ciudad Universitaria, Córdoba 5000, Argentina

Received 27 April 2009; accepted 4 September 2009

DOI: 10.1002/pola.23717

Published online 5 November 2009 in Wiley InterScience (www.interscience.wiley.com).

ABSTRACT: Heterogeneous networks of ethylene glycol dimethacrylate and 2-hydroxyethyl methacrylate [poly(EGDMA-co-HEMA)] were synthesized by suspension polymerization using different EGDMA contents and agitation speeds. The networks were activated with epichlorhydrine (Ech) or 1,4-butanediol diglycidyl ether (BDGE), and then hexamethylenediamine (HMDA) or ethylenediamine (EDA) were conjugated to the support by coupling reaction. Here, a higher alkyldiamine concentration and temperature, and a longer reaction time led to higher yields. Amino ligands of the support III were used to analyze their adsorption performance of bovine serum albumin (BSA) from the adsorption kinetic. A more external location of HMDA amino ligands into network led to get the maximum adsorption in a time shorter than that with EDA. Due to its bigger size, the HMDA molecule was attached mostly to the network surface between larger pores, which favored a faster protein adsorption. When derivatives containing BDGE were compared, the EDA ligand displayed a BSA retention higher than that with HMDA, because a shorter separation between the ammonium groups along the spacer arm yielded a stronger electrostatic attraction on the protein. Clearly, the balance obtained between the pores system and the reagents molecular structure used in the formation of Ech-HMDA generated the most efficient BSA adsorption. © 2009 Wiley Periodicals, Inc. *J Polym Sci Part A: Polym Chem* 47: 6771–6782, 2009

Keywords: albumin; HEMA; heterogeneous polymers; ion exchangers; macroporous polymers; structure-property relations

INTRODUCTION

Porous solid materials are important in many fields of modern science and technology including ion exchanger, molecular separation, as well as catalysis, chromatography, microelectronics, and energy storage.^{1–5} The aim of most research in the field of ion exchange is to enhance the functional properties of the support such as selectivity, capacity, and rate, with direct impact on the

applicability of resins.⁶ Derivatives with alkyl amines have been used in affinity chromatography for the purification of amino oxidases⁷ and other proteins with affinity for the amino group.^{8,9} The efficiency of all the aforementioned processes is affected by both the type and concentration of chelating groups and the morphological features of the support because the molecules diffuse interconnected cavities of different size. Moreover, adsorbents need to introduce a spacer arm between the ligand and the support surface¹⁰ to enhance the accessibility of the ligand, and binding has been strongly recommended in the field of conventional affinity chromatography. Ligand is

Correspondence to: M. C. Strumia (E-mail: mcs@fcq.unc.edu.ar)

Journal of Polymer Science: Part A: Polymer Chemistry, Vol. 47, 6771–6782 (2009)
© 2009 Wiley Periodicals, Inc.

separated from the matrix for the distance of a spacer length, which also provides an increase in protein (substrate) flexibility compared with the direct coupling with the matrix.¹¹ However, an ideal spacer arm should have a proper length (at least three atoms), no active center which could cause nonspecific adsorption and bifunctional groups to react with both solid support and ligand.¹⁰ An increase in the length of the spacer corresponds to an increase in its rotational flexibility, which can eventually lead to formation of structures where the ligand is interacting with the support. In particular, if the spacer is hydrophilic and rigid, the structure more favored will result in an extended spacer and solvated ligand.¹² Dephillip et al.¹³ examined the effect of spacer arm length on protein retention on a cation-exchange adsorbent, with the greatest retention seen for the adsorbent with no spacer arm.

On the other hand, the synthesis of macroporous networks with interconnected pores that allow the diffusion of large solutes and that provide large surface area for further chemical modifications is a matter of discussion in several research groups.^{14–17} In previous works, we have analyzed the construction of matrices through suspension polymerization, examining several reaction conditions such as type of monomers, diluents, crosslinker content, and stirring speed in the development of the porous structure.^{18–20} Therefore, in this research amino ligands were attached to the network from the construction of different spacer arms, and the performance of BSA adsorption on the amino ligands obtained was then analyzed. Four macroporous networks (R) with different morphological structures were synthesized from the variation of the EGDMA content and the stirring speed. Hydroxyl groups present in the base support were reacted with the oxirane groups of BDGE or Ech, and then EDA or hexamethylenediamine (HMDA) were attached through alkyldiamine coupling reaction, which takes place on the epoxy-activated support. The optimization of above step ways of derivatization allowed attaining amino derivatives with the best properties, which were able to bind BSA by electrostatic interaction.

EXPERIMENTAL

Reagents and Equipments

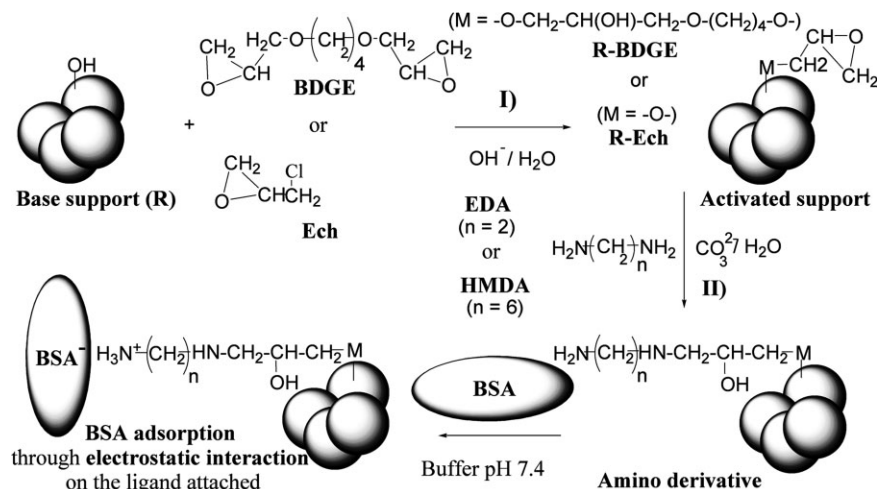
The following reagents were purchased and used as received: 2-hydroxyethyl methacrylate

(HEMA), ~95(GC) Fluka-Switzerland; ethylene glycol dimethacrylate, (EGDMA), >97(GC) Fluka-Switzerland; poly (vinylpyrrolidone) (PVP), Kollidone 90, Fluka-Switzerland; cyclohexane (Cyc), p.a. Anedra-Argentina; hydroxy-methyl-aminomethane (Tris), p.a. Anedra-Argentina; hydrochloric acid (HCl), Merck-Germany; albumin bovine serum (BSA), p.a. Merck-Germany; 1,4-butanediol diglycidyl ether (BDGE), 62% by GC, Sigma-USA; epichlorhydrine (Ech), p.a. Riedel de Haen-Germany; potassium chloride (KCl), p.a. Mallinckrodt-USA; ethylenediamine (EDA), p.a. Carlo Erba-USA; hexamethylenediamine (HMDA), purified by distillation at reduced pressure at 100 °C/20 mm Hg, Fluka-Switzerland; benzoyl peroxide (BPO), Riedel de Haen-Germany, purified by crystallization from chloroform/methanol mixture, and dried at room temperature before use.

Polymeric networks were synthesized using a magnetic stirrer “04644-Series Digital Hot Plate/Stirrer (Cole Parmer-USA)”. At the Department of TEMADI, CAB-CNEA (Bariloche-Argentina), an “Auto-Pore 9220 Micromeritics Inst. Corp” was used in the characterization of dry networks by mercury intrusion porosimetry. Using this technique, pore size distribution ($dV/d \log D$), specific pore volume (V_p), specific surface area (S_s), average pore size (D_A), apparent density (δ_0) and porosity percentage ($P\%$) of dry networks were obtained (pore diameter range: $4-4 \times 10^5$ nm). The true density value (δ_2) of the base-supports was determined through helium pycnometric density, using an “Autopycnometer 1320-Micromeritics Inst. Corp”. Scanning electron microscopy (SEM) assay was performed on an “EVO 40 XVP, LEO (2003) apparatus”, at the laboratories in Centro Regional de Investigaciones Básicas y Aplicadas de Bahía Blanca (CRIBBAB), CONICET-Argentina. The BSA concentration was obtained by UV-vis spectroscopy from measurement of absorbance at 280 nm using a spectrophotometer UV-vis Shimadzu UV-260.

Synthesis of the Polymeric Network

Polymer beads were prepared by suspension polymerization in a 250-mL round bottom flask equipped with a reflux condenser and a magnetic stirrer. The reaction mixture was heated at 85 °C in a bath of water and stirred for 2 h with a magnetic stir bar 3-cm long and 1.5-cm wide. Networks were synthesized using a ratio of 25 mol % of crosslinking agent (EGDMA) to total vinyl



Scheme 1. Attaching of the amino ligands to the surface networks through spacer arms. Base support modified with oxirane groups employing an activation reaction (I); an alkyldiamine coupling reaction (II) then took place. Amino derivatives attained were used as adsorbents of the BSA protein.

monomers in the reaction mixture under a stirring speed of either 450 or 750 rpm. To obtain about 10 g of dry polymer, in the reaction mixture a mole ratio of 3.0:1.0:9.3:2.5:3 $\times 10^2$ of HEMA (6.2 mL), EGDMA (3.2 mL), Cyc (17.2 mL), and water (77.0 mL), respectively, was used. Likewise, in all cases, the free radical initiator BPO (0.411 g, 2.44 mol %) was also added, using PVP (0.777 g, 10 mg/mL of total mixture) as a suspension stabilizer. Afterward, the resulting polymer beads were exhaustively washed with distilled water and then with ethanol. This procedure removed the porogenic diluent, PVP, and some unreacted monomers. Next, the samples were dried in an oven at 70 °C to reach a constant mass. The yield reaction was calculated as the percentage of dry matrix obtained versus the total grams of vinyl monomers used. Finally, the assays of network swelling in water, FTIR, SEM, and mercury intrusion porosimetry characterized the network. Moreover, networks with 6 and 33 mol % of EGDMA were attained using the same procedure described previously and a stirring speed of 450 rpm.

Preparation of the Adsorbents

Activation Reaction of the Matrix

The hydroxyl groups of each poly(EGDMA-co-HEMA) network was reacted in basic aqueous solution with the oxirane groups of BDGE to obtain terminal oxirane groups attached to the polymeric chains (Scheme 1). First, a sample

(3.00 g) of dry network (R—OH) was swollen in dimethylformamide (5.80 mL/g) for 24 h at room temperature, and was then mixed with BDGE or Ech and a 0.74 N NaOH solution yielding an epoxy-activated support (R-oxirane). Networks I, II and IV, and III presented a hydroxyl group content informed like a mole ratio of 0.9, 1, and 1.4, respectively. The amount of hydroxyl groups per gram of dry network was considered in reference to the HEMA content used during polymerization. Then, a mole ratio was used 1:12:0.5 of hydroxyl groups, oxirane and base, respectively, under stirring for 7.5 h at room temperature. Finally, the epoxy-activated supports were purified through exhaustive washes of water and ethanol, and dried until reaching a constant weight. Next, the amount of oxirane groups per gram of dry product was determined using a colorimetric acid–base titration.²¹

In a similar procedure to the above described, in an attempt to enhance the Ech and BDGE yield, the support III was also activated using a mole ratio of 1:2:3 of hydroxyl groups, oxirane and base, respectively. Here, a 10 N NaOH solution was employed in the reaction mixture.

Amine Coupling on Epoxy-Activated Supports

Amino ligands were attached to the epoxy-activated networks by reaction of the pendant oxirane on polymeric backbone with an amino group of the alkyl diamine (Scheme 1). The epoxy-activated matrix (2.00 g) was swollen in water

(5.40 mL/g) for 24 h at room temperature and then mixed and reacted for 12 or 24 h at 60 °C with HMDA or EDA dissolved in a 2 M aqueous solution of Na₂CO₃. Here, a mole ratio of 1:(5, 10 or 40):72 of epoxy:alkyldiamine:Na₂CO₃, respectively, was used in the reaction mixture. The amine derivatives were filtered, washed with 300 mL of distilled water, 0.1 N acetic acid solutions (200 mL), and then again with distilled water until reaching the supernatant pH 7. Once the products were purified and dried, the amino group content was determined by colorimetric acid–base titration.²²

Methods

Analysis of the Network Swelling in Water

The assays of network swelling were carried out in distilled water (pH 6). In this process, a polymer sample (0.10 g) was left in contact with water (excess) in a special funnel (with a very small hole) into a closed chamber for 24 h followed by a further 24 h drainage in the same closed chamber. Then, the wet sample was weighed on an analytical scale at different times (every 15 s for 7–8 min after the sample was removed from the chamber). The data were processed using a plot of swollen sample weight (g) versus evaporation time (s), where the swollen mass of the sample (W_{sw}) from curve extrapolation was taken at time zero. Subsequently, the samples were dried in an oven at 70 °C for 48 h, and then weighed to obtain the dry sample weight (W_{dry}). The equilibrium weight swelling ratio (Q_w) was also calculated according to eq 1.

The equilibrium volume swelling ratio (Q_v) was obtained from the ratio of the volume (eq 2) of the sample in swelling equilibrium state (V_{sw}) and the volume of the sample in dry state (V_{dry}). The measurement of V_{sw} and V_{dry} value was performed using graduated tubes after the dry sample (particle size range, 40–70 mesh) had been soaked for 24 h in excess of distilled water. The assays were carried out four times and the results generally showed an error less than 8 %. The data of the Q_w obtained, where the swelling liquid density ($\delta_1 = 1.00$ g/mL) and the true polymer density ($\delta_2 = 1.283$ g/mL), were used to calculate the network porosity percentage in swollen state, expressed in eq 3.²³ The network morphology in swollen state was analyzed employing relative values of Q_w and Q_v (eqs 1 and 2) of heterogeneous networks, which provide information about

the distribution of the diluent between the gel and the diluent phases at the end of the network formation process.²⁴

$$Q_w = W_{sw}/W_{dry} \quad (1)$$

$$Q_v = V_{sw}/V_{dry} \quad (2)$$

$$P(\%) = \frac{(Q_w - 1)/\delta_1}{[(Q_w - 1)/\delta_1] + 1/\delta_2} \times 100 \quad (3)$$

Quantification of Functional Groups on Polymeric Chain

The quantification of oxirane groups was performed by the pyridinium chloride method,²¹ which is a retrocession titration. The epoxy-activated matrix (0.1 g) was placed into an Erlenmeyer flask with 2.0 mL of 0.05 N pyridinium chloride solution and left under agitation in a reflux system near 90 °C for 45 min. Then, the reaction mixture was titrated at room temperature with 0.05 N NaOH aqueous solutions, employing phenolphthalein as a colorimetric indicator.

On the other hand, the amount of amino groups in the amino derivatives was also determined by acid–base colorimetric titration. Modified polymer (0.1 g) with terminal amino groups was kept in an Erlenmeyer flask with 4.0 mL of HCl aqueous solution (0.01 N) under stirring at room temperature for 1 h. The acid protons react with the amino groups of the derivative and then the proton content in the mixture decrease. Next, the supernatant (1.0 mL) was titrated with a 0.01 N NaOH aqueous solution up to the color change of phenolphthalein.²²

BSA Adsorption on the Derivatives of the Support III Containing Amino Ligands

The alkyldiamine coupling reaction was examined to achieve the best reaction condition, where epoxy-activated networks with either BDGE or Ech were modified with terminal amino groups. Considering the suitable morphological properties of the base support III, such as high values of S_s , V_p and porosity (Table 1), it was selected for its derivatization, investigating then the performance of BSA adsorption on the attained amino derivatives. Using a system batch with 15.0 mL of buffered-BSA solution (0.45 g/L), the kinetics of

Table 1. Physical Properties of the Networks Belonging to Their Swollen and Dry State

R	EGDMA							
	(mol %)	Q_w^a	Q_v^a	P^a (%)	P^d (%)	V_p (mL/g)	S_s (m ² /g)	D_A^e (nm)
I ^b	6	3.82	1.59	78	71	0.90	3.4	1,066
II ^b	25	6.22	1.20	87	83	1.26	5.3	956
III ^b	33	6.41	1.07	87	83	1.57	9.6	656
IV ^c	25	6.27	1.14	87	84	1.45	4.3	1,360

Swelling assay.

^aIn water (eqs 1–3) of the networks (R) obtained at 450.^bor 750 rpm.^cOf stirring speed. The porosity percentage.^dOf the dry networks was attained from mercury intrusion porosimetry. The average pore diameter.^e($D_A = 4000 \times V_p/S_s$) corresponds to the pore size range of $50-1 \times 10^4$ nm.

BSA adsorption on amino derivatives of the support III (Table 2) were analyzed. In this assay, 0.2 g of a dry sample of the amino derivative was maintained under stirring (200 rpm) at room temperature. The BSA concentration of the supernatant solution was measured as a function of the adsorption time on support. For the first 2 h at intervals of 20 min, and every 30 min for the remaining 3 h, the sample was centrifuged and an aliquot of 2.0 mL of BSA supernatant solution was taken, and its absorbance was measured twice. Moreover, this procedure was carried out twice with each support, and then the BSA adsorption in mg per gram of dry support was attained. The BSA concentration was obtained from measuring the absorbance at 280 nm, using an extinction coefficient of $0.615 \text{ cm}^{-1} \text{ L g}^{-1}$ calculated from an appropriate calibration curve. UV-visible spectra were recorded with a Shimadzu

recording spectrophotometer UV-260. The buffer used to carry out the studies of BSA adsorption was chosen from a previous work.²⁵ Then, a 0.01 M of Tris-HCl solution at pH 7.4 was prepared using an aqueous solution 0.1 M of KCl as solvent.

RESULTS AND DISCUSSION

Heterogeneous networks (I–IV) of poly(EGDMA-co-HEMA) were synthesized by suspension polymerization, and characterized by mercury intrusion porosimetry, SEM, FTIR, and study of network swelling in water. Modification reactions on matrix were carried out firstly substituting the hydroxyl groups present on polymeric backbone by oxirane groups, and then by amino groups in other pathway (Scheme 1). The amino derivatives

Table 2. Amino Ligands Attached to the Base-Support (III) Through Different Spacer Arms

Amino Derivative	Spacer Arm	Oxirane Group Content ($\mu\text{mol/g}$)	Terminal Amino Group ($\mu\text{mol/g}$)	Coupling Reaction Yield (mol %)	Maximum Adsorption of BSA ^c (mg/g)	Spacer Atoms Number
1	BDGE ^a -EDA	65 ± 7	31 ± 6	47	9.6 ± 0.4	16
2	BDGE ^a -HMDA		48 ± 4	74	8.7 ± 0.3	20
3	Ech ^b -EDA	82 ± 6	52 ± 6	63	7.6 ± 0.3	7
4	Ech ^b -HMDA		79 ± 8	96	10.2 ± 0.5	11

^aEpoxy-activated matrices were attained employing a mole ratio 1:12:0.5 of hydroxyl, BDGE, and base, respectively.^bHowever, a mole ratio 1:2:3 was used to prepare the Ech derivatives.^cMaximum degree of BSA adsorption achieved on the amino derivatives was calculated as the data range average corresponding to the plateau of each curve in Figure 5.

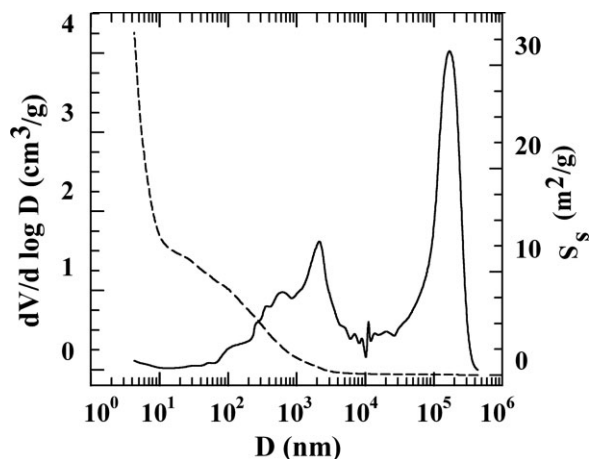


Figure 1. Pore size distribution (solid line) and specific surface area (dash line) of the heterogeneous network of the support III. These curves were attained from the assays of mercury intrusion porosimetry performed on the dry sample.

were employed as adsorbents in an adsorption study of a model protein such as BSA to investigate the role of the spacer arm in the adsorption performance.

Synthesis and Characterization of the Networks

Three heterogeneous networks (I–III) of poly-(EGDMA-*co*-HEMA) were prepared by suspension polymerization using an agitation of 450 rpm and different contents of EGDMA (6, 25, and 33 mol %). Moreover, the agitation speed was also varied during network formation, and a fourth matrix IV was synthesized using a 25 mol % of EGDMA at 750 rpm. These base supports consisted of white, smaller, densely crosslinked microspheres forming a porous mesh, which in turn formed larger macrospherical beads. In all cases, the polymerization yield was between a 95 and 98 % w/w. In a previous work²⁰ these networks have just been characterized, where the increase of the EGDMA concentration was found to lead to an earlier phase separation during polymerization. Therefore, networks with a higher crosslinking degree ($\sim 1/Q_v$), S_s value and porosity (Table 1) were attained. It is known that during polymerization, the nuclei are generated first, which are nonporous and constitute the highly crosslinked regions of the network.²⁴ Beads contain large agglomerates of microspheres (50–200 nm) which consist of smaller nuclei (10–20 nm) fused together. An earlier phase

separation yields nuclei that are more rigid and a higher aggregation of smaller microspheres, showing a network with a lower average pore size (D_A) and a more stable pore system.²⁴ This behavior can be seen (Table 1) from the porosity, which in swollen state was about 4 % higher than that in dry state. This small variation in porosity supports the stability of the network porous structure. On the other hand, the increase in coalescence frequency led to the decrease in the stabilizer molecules, which generated an increment in drop size. Large fused aggregates of microspheres were formed with additional loss of small pores as the stirring was increased, attaining also a higher V_p , and a slight decrease in the surface area (Table 1). Figure 1 exhibits as an example a curve of bimodal pore size distribution ($dV/d \log D$) against pore diameter (D) of a base support, whose porous architecture demonstrates the achievement of a heterogeneous network. Figure 1 also shows that the pore system (50 nm–10 μm) belonging to the interconnected microspheres has a high specific surface area, whereas no area is seen for the pore size distribution (10–400 μm) of the above particle agglomerates. This is particularly important for the analysis of the specific surface area of a support. Moreover, the SEM micrograph (Fig. 2) of the network confirms the formation of a heterogeneous surface corresponding to conglomerates of spherical particles (microspheres) and their aggregates. In this case, the network micrograph displays a typical example of a polymer bead obtained from suspension polymerization.

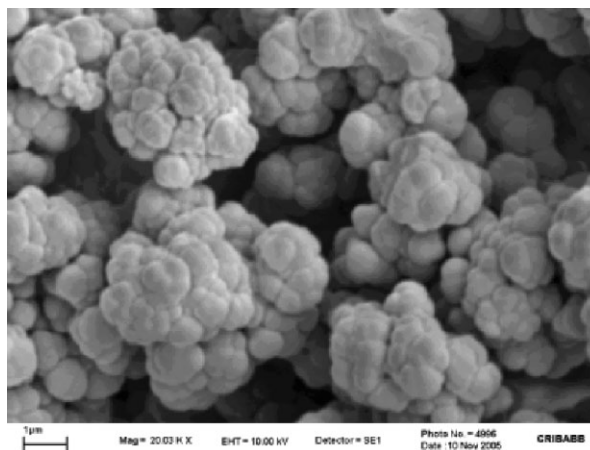


Figure 2. Micrographs corresponding to the surface and interior of a polymer bead attained from suspension polymerization. Magnification and its scale are displayed inside the photograph.

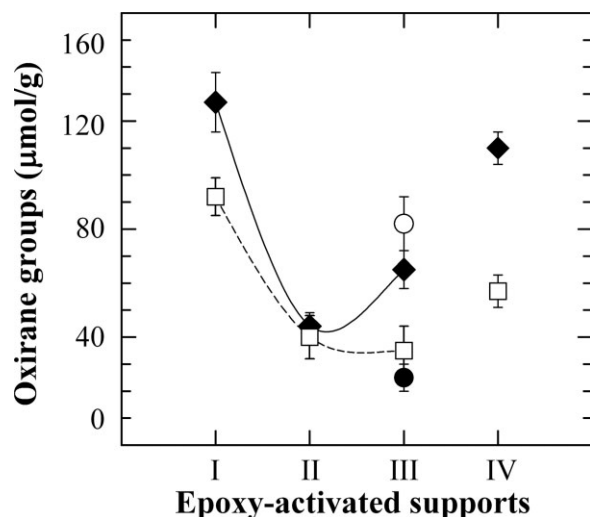


Figure 3. Influence of the network morphology on activation reaction. Base-supports I–III synthesized at 450 rpm have a content of hydroxyl group near 94, 75 and 67 mol %, respectively, while network IV with 75 mol % of hydroxyl group is attained at 750 rpm. The following symbols belong to the epoxy-activated derivatives of BDGE (black diamond) and Ech (white square), which were obtained from a mole ratio (1:12:0.5) of hydroxyl, oxirane and base, respectively. When a reagent mole ratio 1:2:3 was used in similar reaction conditions to the above described, other derivatives of BDGE (black circle) and Ech (white circle) were attained.

Modification of the Support – Attaching of the Amino Ligand Through a Spacer Arm

Synthesized networks were modified first through an activation reaction with oxirane groups and then by an alkyldiamine coupling reaction (Scheme 1). Several reaction conditions were employed to optimize these reactions in an attempt to achieve adsorbents with the best properties.

Optimization of the Activation Reaction

Poly(EGDMA-co-HEMA) networks (I–IV) were activated in basic aqueous solution through reaction of the hydroxyl groups present on the backbone with oxirane groups of either BDGE or Ech (Scheme 1), examining two reaction conditions. The activation reaction was first carried out using a mol ratio 1:12:0.5 of hydroxyl groups, oxirane and base, respectively. Figure 3 shows a typical U-shape activation curve, where the Ech derivatives and BDGE present a similar behavior

related to two opposed effects described in a previous work by Gomez and Strumia.²⁰ One effect is characterized by the amount of hydroxyl groups present in the matrix; the other relates to the diffusion into the network together with its accessible surface. For networks with an EGDMA content from 6 to 25 mol %, the number of hydroxyl groups decreases (Fig. 3) generating a smaller amount of pendant oxirane groups in the derivatives. However, from 25 to 33 mol % the diffusion and capacity of the network become more important and the reaction activation increases (Fig. 3), because the yield depends mainly on the V_p value (Table 1). Figure 3 also shows that the base-support IV synthesized from a higher agitation speed presents a large activation performance than network II due to a higher diffusion as network IV shows (Table 1) a bigger value of V_p and D_A . In similar reaction conditions (2.2), other epoxy-activated derivatives of network III were obtained employing a mol ratio 1:2:3 of hydroxyl group, Ech or BDGE, and base, respectively. Figure 3 also shows that in this second reaction condition, the activation yield of the Ech derivative achieves a value near 80 $\mu\text{mol/g}$, while the BDGE derivative yields 25 $\mu\text{mol/g}$. A higher mol ratio from base to Ech increased the nucleophile content in the reaction mixture because the hydroxyl group shifts its equilibrium toward the conjugated base, also increasing the activation yield. Clearly, for each activation condition employed, the molecular structure of the reagents has favored the performance of either BDGE or Ech, without disregarding the differences observed in the reaction mechanism.

Coupling Reaction of Alkyldiamines on the Activated Supports

The pendant oxirane groups of the epoxy-activated supports were reacted in a basic aqueous solution with the amino group of an alkyldiamine such as EDA or HMDA, attaining also the amino ligand attached to the support (Scheme 1). Several conditions of coupling reaction such as reagent ratio and reaction time were varied on epoxy-activated supports of BDGE. Figure 4 shows that when longer reaction time is used, the system reaches its equilibrium and a higher yield is then achieved. Moreover, a higher concentration of EDA as well as HMDA in the reaction mixture (Fig. 4) leads to the highest yield, the alkyldiamine concentration being clearly the driving force of the molecule diffusion toward the interior

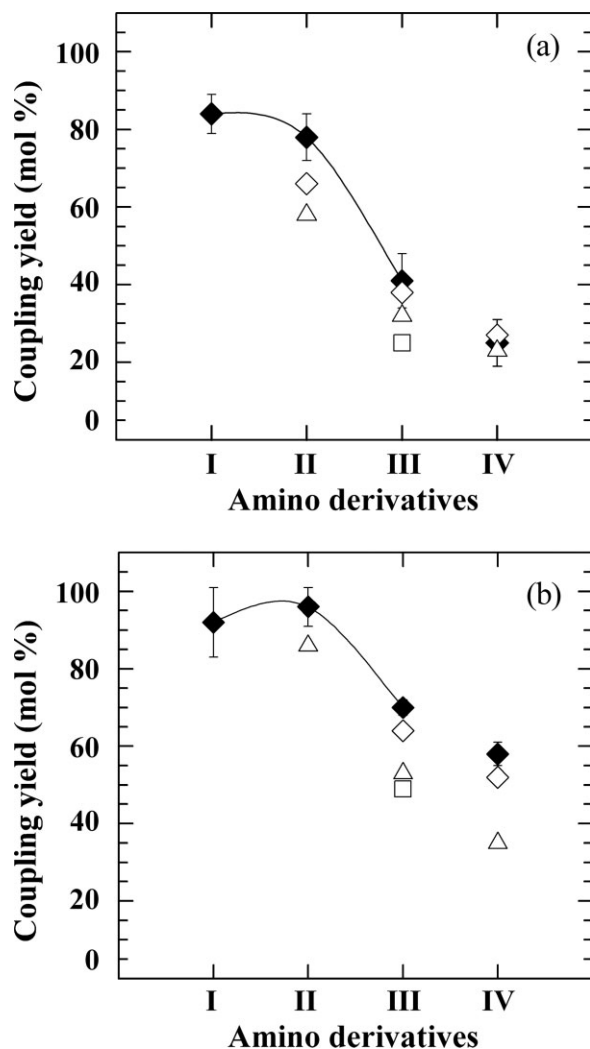
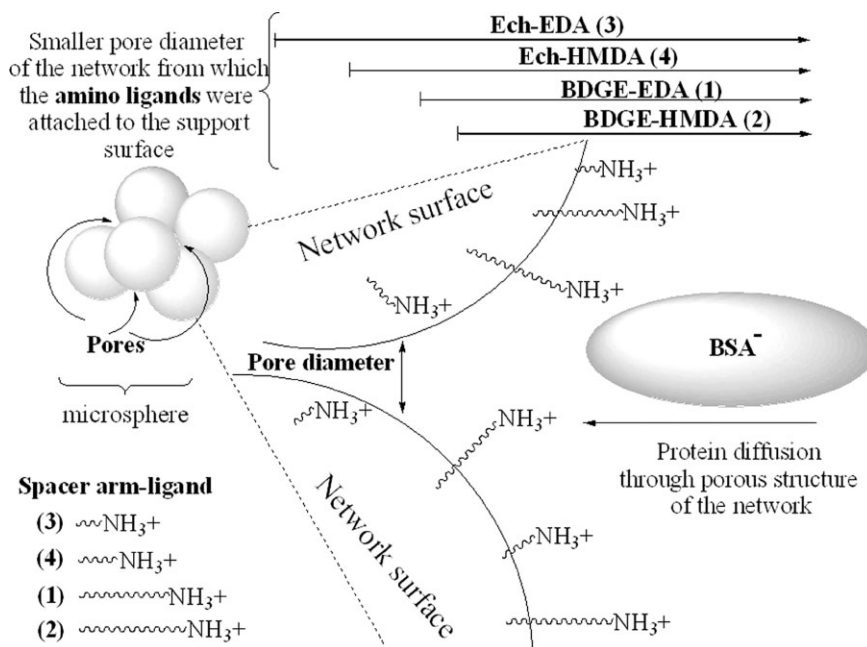


Figure 4. Amino derivatives of EDA (a) and HMDA (b) obtained through the reaction of alkyldiamine coupling carried out on BDGE-activated supports. Effect of the alkyldiamine concentration on the reaction yield for 24 h, using an alkyldiamine mol ratio of 5 (white square), 10 (white triangle) or 40 (black diamond) in each case. Products generated from an alkyldiamine mol ratio of 40 (white diamond) and a reaction time of 12 h.

of the network. Additionally, Figure 4 confirms that the yield of alkyldiamine coupling decreases from support I to IV when the reactivity of the BDGE derivatives is compared. This behavior is related to the decrease in the network expansion degree and the oxirane group content (Table 1 and Fig. 3). Since the base supports of the epoxy-activated derivatives III and IV display (Table 1) a higher crosslinking density ($\sim 1/Q_v$) and porosity, the largest extension of the coupling reaction

was carried out on the accessible oxirane groups of the support surface. These pendant oxirane groups able to react were mostly attached to the network surface between pores equal to or larger than the reagent from which the former were generated (Scheme 2).²⁰ Therefore, the space disposition of the pendant oxirane groups and the accessibility of the alkyldiamine into the support have controlled the performance of the coupling reaction. Figure 4 indicates that in all the cases the yield of HMDA coupling is higher than EDA, which could be related to the compatibility of each alkyldiamine with the reaction center. Hydrophobic character of the pendant oxirane groups of the BDGE derivatives may be limiting its interaction with the amino group. Thus, a higher number of methylene groups provides HMDA with a better compatibility with the oxirane groups, which enhances the ability of the nitrogen atom as nucleophile to access the reaction center. Probably the molecular structure of the alkyldiamine defines a compromise ratio between polarity and accessibility.

Although the ligand content is an important topic to consider in chromatographic supports, the adsorption of a large biological substrate is usually a phenomenon that occurs on the adsorbent surface. Adsorption performance of supports with a smaller crosslinking density is strongly dependent on the network expansion degree, which may be affected by different conditions such as temperature, pH, and ionic power. Therefore, adsorbents constituted by stable pore systems whose networks present high porosity, S_s and rigidity, are recommended in chromatography. Taking into account that the base-support III showed (Table 1) the best morphological properties, its epoxy-activated derivatives containing the highest functionality were employed in the preparation of the four amino adsorbents (1–4). Table 2 shows that the content of terminal amino groups of the HMDA derivatives (2 and 4) is higher than that in the EDA derivatives (1 and 2). This behavior is supported by the effect of the alkyldiamine compatibility described above for the coupling reaction. In addition, Table 2 reveals that the alkyldiamine coupling yield of the derivatives 3 and 4 containing Ech is higher than that with BDGE (1 and 2). A larger segment of methylene groups in the latter led to a bigger nonspecific interaction with the support, which decreased the performance of the coupling reaction.¹²

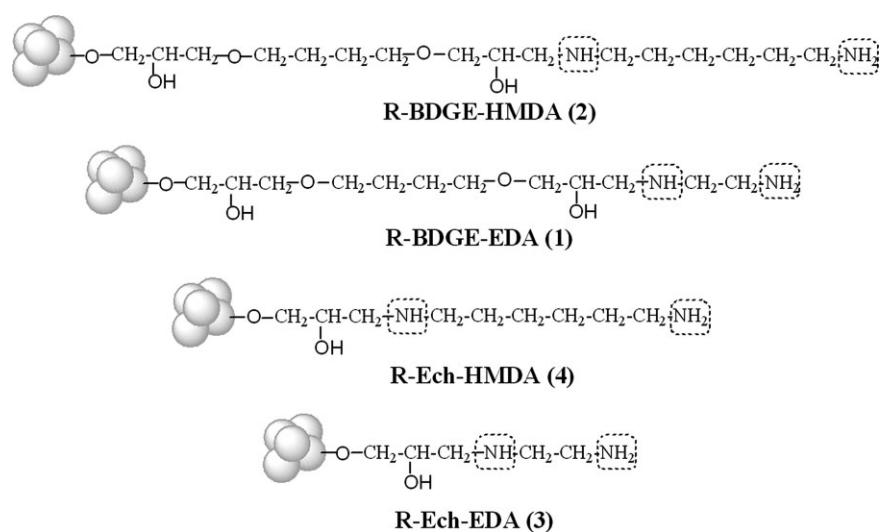


Scheme 2. Final location of amino ligands on the network surface into porous structure as a function of the reagent size used in the spacer arm construction. Influence of the substrate size on its diffusion through pores, which limits the access toward the interaction centers.

Adsorption of BSA on the Amino Ligands Attached Through Different Spacer Arms

Although the length of the arm spacer is an important factor that needs to be considered in relation to the degree of substrates adsorption, the primary focus in heterogeneous networks is far more complex. Here, the performance of BSA

adsorption on the amino ligands is governed by the ligand content and the support accessibility, the latter depending on the location of the interaction center inside the porous structure of the matrix. Support III was selected as a base matrix to attach the amino ligands through different spacer arms (Scheme 3) using the most favorable reaction conditions because it displayed the highest



Scheme 3. Molecular structure of the spacer arms built on the support III (R). These amino derivatives (1–4) present amino groups separated along the spacer arm by different lengths.

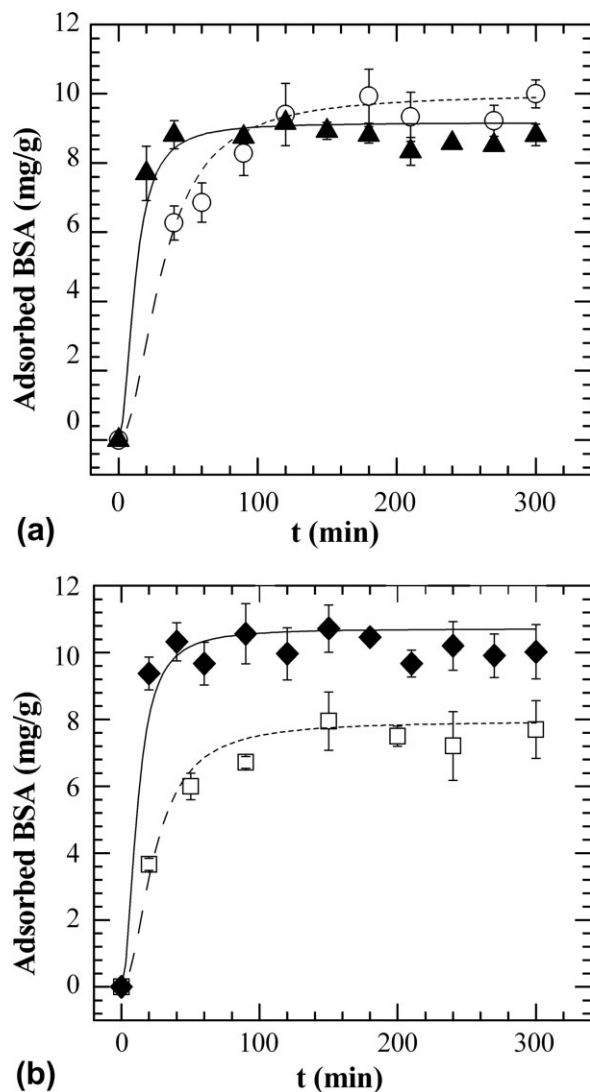


Figure 5. Kinetics of BSA adsorption on the amino derivatives of the support III (1–4) corresponding to the following spacer arms: (a) BDGE-HMDA (black triangle), BDGE-EDA (white circle), and also (b) Ech-HMDA (black diamond) and Ech-EDA (white square).

S_s , V_p and porosity (Table 1), which are morphological properties required for chromatographic adsorbents. Here, the kinetics of BSA adsorption on four amino derivatives was examined using a batch-wise (Fig. 5, Table 2). Each adsorbent (1–4) was mixed with a buffered solution of BSA at pH 7.4 and kept under stirring at room temperature. BSA concentration in the supernatant was obtained from absorbance measurement at 280 nm by UV-vis spectroscopy. Figure 5 shows that the BSA adsorption curves of the HMDA adsorbents 2 and 4 reach the plateau at a shorter time (50 min) than with the EDA supports 1 and 3, which is related to the protein accessibility to-

ward the interior of the network (Scheme 2). The protein enters the network until a pore size is equal to or higher than that acquired by the protein conformation, and then BSA interacts with the ligand. Due to its size, the HMDA molecule was attached mostly to the support surface between larger pores (Scheme 2) than those in EDA, showing also the protein an easier access on the former. This tendency is consistent with a more external disposition of the alkyldiamine coupled to the support surface explained above in 3.22, which controls the protein adsorption. The maximum capacity of BSA adsorption of the amino derivatives displays the following decreasing order: 4 (10.2 mg/g), 1 (9.6 mg/g), 2 (8.7 mg/g), and 3 (7.6 mg/g) (Table 2). Although the capacity of BSA adsorption of these adsorbents is lower than that found by other authors,²⁶ the BSA retention values are enough high, presenting these derivatives an interesting performance. Clearly, the degree of BSA adsorption of the HMDA amino ligands 2 and 4 has been controlled by the amino group content, showing the longer spacer arm an adverse effect in the process. The influence of the molecular structure of spacer arm was also observed in the yield of coupling reaction (Table 2), which was attributed to a bigger non-specific interaction between BDGE and the support (section 3.22). Since the BSA adsorption depends largely on the accessible functionality of the support, a higher amino group content of the HMDA derivatives and a more external location led to attain a faster saturated protein capacity (Scheme 2).

Although the amino ligand 1 displays a lower amount of the amino group (Table 2) when the EDA derivatives are compared, it presents a higher available functionality and a better BSA adsorption performance than that of the adsorbent 3. The latter is attached to the support surface from pores of a narrower diameter, as it is built from reagents of a smaller size, which diffuse easily into the network (Scheme 2). Therefore, although the spacer arm three has a higher functionality, a percentage of this one is attached to the network surface between a narrower pore diameter, which gives a hidden functionality where the protein does not have access. On the other hand, the separation length between the nitrogen atoms charged along the spacer arm has controlled the protein adsorption.²⁷ Scheme 3 indicates that the molecular structure of EDA has two amino groups separated by a distance shorter than that found in HMDA. It is known that the protonation of the first amino makes it more

difficult to protonate the second amino group in small alkyldiamines because of the increase in the overall positive charge of the molecule.²⁷ However, the two positive charges of the ammonium groups present a higher attraction force over the negatively charged protein and a lower amount of methylene group decreases the nonspecific interactions with the support. The last effects explain the better performance of BSA adsorption found for EDA (1) at pH 7.4 (Table 2) when the amino derivatives 1 and 2 containing BDGE were compared.

CONCLUSIONS

Macroporous networks (I–IV) of poly(EGDMA-co-HEMA) were synthesized from suspension polymerization using different EGDMA contents and agitation speeds. The networks were activated with oxirane groups of BDGE or Ech, where a mole ratio of 1:12:0.5 of hydroxyl, oxirane group and base, respectively, favored to the activation reaction with BDGE, while for Ech a mole ratio of 1:2:3 was more successful. Then, amino ligands of EDA or HMDA were conjugated to the support by coupling reaction, where a higher alkyldiamine concentration and temperature, and a longer reaction time led to higher yields. The amino ligands of the support III were selected to analyze their performance of BSA adsorption from the adsorption kinetic. The maximum capacity of BSA adsorption of the amino derivatives shows the following decreasing order: 4 (10.2 mg/g), 1 (9.6 mg/g), 2 (8.7 mg/g), and 3 (7.6 mg/g). Moreover, it was found that the HMDA ligands reached the plateau in a shorter time than with EDA. Due to its higher size, the HMDA molecule was attached in a more external location to the network surface between larger pores, which gave the protein a faster access to the interaction center. Here, the performance of amine ligands is governed by the accessible functionality of the matrix, which depends on the spacer arm length and its location into the network, and also on the content and effective charge of the amine ligand. These factors are ruled by the reagents size from which the spacer arm is built and the pore system of the network. A reagent with a smaller size leads to a location of the spacer arm from a narrower pore diameter, and then a higher surface area is available, yielding a higher amine group content. However, the protein size controls its diffusion into the network and defines the accessible

functionality of the support. On the other hand, the existence of hydrophobic groups along BDGE spacer arm decreases the performance of BSA adsorption because of the unspecific interaction of the spacer arm with the support. Moreover, a shorter separation among the ammonium groups of BDGE-EDA results in a higher attraction power on the negatively charged protein, showing a BSA adsorption more successful than that found in BDGE-HMDA. Clearly, the balance obtained between the reagent molecular structure and the pores system during the formation of the couple Ech-HMDA generated the most efficient BSA adsorption.

The authors thank the financial assistance of Consejo Nacional de Investigación Científica y Tecnológica (CONICET), Fondo para la Investigación Científica y Tecnológica (FONCYT) and Secretaría de Ciencia y Técnica de la Universidad Nacional de Córdoba (SECYT-UNC).

REFERENCES AND NOTES

- Vlakh, E. G.; Tennikova, T. B. *J Chromatogr A* 2009, 1216, 2637–2650.
- Miletić, N.; Vuković, Z.; Nastasović, A.; Loosa, K. *J Mol Catal B* 2009, 56, 196–201.
- Yuan, Z. Y.; Su, B. L. *J Mater Chem* 2006, 16, 663–677.
- Sun, W.; Kherani, N. P.; Hirschmann, K. D.; Gadeken, L. L.; Fauchet, P. M. *Adv Mater* 2005, 13, 1230–1233.
- Rohr, T.; Hilder, E. F.; Donovan, J. J.; Svec, F.; Frechet, J. M. J. *Macromolecules* 2003, 36, 1677–1684.
- Ismail, I. M.; Nogami, M.; Suzuki, K. *Sep Purification Technol* 2003, 31, 231–239.
- Houen, G. *J Biochem Biophys Methods* 2001, 49, 189–197.
- Kecili, R.; Say, R.; Ersoz, A.; Yavuz, H.; Denizli, A. *Sep Purification Technol* 2007, 55, 1–7.
- Trodler, P.; Nieveler, J.; Rusnak, M.; Schmid, R. D.; Pleiss, J. *J Chromatogr A* 2008, 1179, 161–167.
- Zou, H.; Luo, Q.; Zhou, D. *J Biochem Biophys Methods* 2001, 49, 199–240.
- Platonova, G. A.; Tennikova, T. B. *J Chromatogr A* 2005, 1065, 19–28.
- Busini, V.; Moiani, D.; Moscatelli, D.; Zomolo, L.; Cavallotti, C. *J Phys Chem B* 2006, 110, 23564–23577.
- Dephillips, P. *Anal Chem* 2004, 76, 5816–5822.
- Grochowicz, M.; Bartnicki, A.; Gawdzik, B. *J Polym Sci Part A: Polym Chem* 2008, 46, 6165–6174.

15. Egger, C. C.; Du Fresne, C.; Raman, V. I.; Schädler, V.; Frechen, T.; Roth, S. V.; Müller-Buschbaum, P. *Langmuir* 2008, 24, 5877–5887.
16. Grosse, M. T.; Lamotte, M.; Birot, M.; Deleuze, H. *J Polym Sci Part A: Polym Chem* 2008, 46, 21–32.
17. Oh, J. K. *J Polym Sci Part A: Polym Chem* 2008, 46, 6983–7001.
18. Gomez, C. G.; Alvarez Igarzabal, C. I.; Strumia, M. C. *Polymer* 2004, 45, 6189–6194.
19. Gomez, C. G.; Alvarez Igarzabal, C. I.; Strumia, M. C. *Polymer* 2005, 46, 6300–6307.
20. Gomez, C. G.; Strumia, M. *J Polym Sci Part A: Polym Chem* 2008, 46, 2557–2566.
21. Lee, H.; Neville, K. *Handbook of Epoxy Resins*; McGraw-Hill: New York, 1967; p 17
22. Kasgoz, H.; Ozgumus, S.; Orbay, M. *Polymer* 2003, 44, 1785–1793.
23. Hradil, J.; Horák, D. *React Funct Polym* 2005, 62, 1–9.
24. Okay, O. *Prog Polym Sci* 2000, 25, 711–749.
25. Zhou, X.; Xue, B.; Sun, Y. *Biotechnol Prog* 2001, 17, 1093–1098.
26. Wang, R.; Zhang, Y.; Ma, G.; Su, Z. *Colloids Surf B* 2006, 51, 93–99.
27. Mehta, A.; Zydney, A. L. *J Memb Sci* 2008, 313, 304–314.